OPTIMIZING ARTEMIS LIBRATION POINT ORBIT STATIONKEEPING COSTS THROUGH MANUEVER PERFORMANCE CALIBRATION

Brandon D. Owens,[*] Jeffrey E. Marchese,[†] Daniel P. Cosgrove,[‡] Sabine Frey,[§] and Manfred G. Bester[**]

The first two spacecraft to orbit Earth-Moon libration points—ARTEMIS P1 and P2—performed a combined total of 67 stationkeeping maneuvers over a period of 10 months. The degree of precision required for these small-scale orbit corrections exceeded the degree that had been obtained on these spacecraft in the years leading up to their Lissajous orbit insertions. Therefore, an effort was undertaken to improve maneuver performance in the initial and preceding months of this stationkeeping experience. This paper includes details of the in-flight calibration techniques used to obtain the improved level of performance for these maneuvers. It expands on previously reported THEMIS/ARTEMIS maneuver calibration techniques and results through discussion of newly uncovered issues with maneuver performance modeling, the introduction of new calibration approaches, and the presentation of stationkeeping data. With these procedures and issue resolutions in place, the operations team routinely reduced maneuver magnitude and phase errors to less than 2 mm/s and one degree, respectively (the minimum maneuver magnitude error was 46.3 µm/s). These error reductions ultimately reduced the total ΔV expenditure during Lissajous orbit operations and gave the maneuver designers the flexibility to vary the amount of time between stationkeeping events from 4.6 days to 14.2 days.

INTRODUCTION

The P1 and P2 spacecraft of the Acceleration, Reconnection, Turbulence and Electrodynamics of the Moon's Interation with the Sun (ARTEMIS) mission—the first two spacecraft to orbit Earth-Moon libration points—were not specifically designed for Earth-Moon libration point orbit operations. These spacecraft were designed for a low Earth orbit mission—the Time History of Events and Macroscale Interactions during Substorms (THEMIS) mission—that had relatively coarse maneuver targeting requirements and a spin stabilization attitude control scheme. Moreover, the insertion of these spacecraft into Lissajous orbit had to occur after this nominal mission (i.e., after several years of spacecraft exposure to the space environment and with largely depleted fuel reserves). As a result of these limitations, considerable effort was required to reduce maneu-

---

ver performance errors to levels sufficient to conduct stationkeeping operations in the least stable libration point orbits ever attempted.

The initial phases of this effort were reported in (Reference 1) and were largely successful in improving maneuver performance to meet the requirements for the low-energy transfer trajectory[2] to get the two ARTEMIS spacecraft to Lissajous orbit and for the extended mission operations of the other THEMIS spacecraft in Earth orbit (i.e., THEMIS-Low). However, special measures—described throughout this paper—would have to be taken in the latter phases of this effort in order to optimize the libration point orbit costs for the ARTEMIS mission. The end result was a calibration process that helped the ARTEMIS mission achieve stationkeeping costs of about 5 m/s per year, which was much less than the ΔV budget for the mission and amount suggested in some prior studies.[3]

BACKGROUND

The two ARTEMIS spacecraft are spin-stabilized and contain four thrusters each.[1] Two of the thrusters (i.e., the side thrusters) are oriented roughly parallel to the spacecraft spin plane while the other two (i.e., the axial thrusters) are oriented roughly normal to the spacecraft spin plane. The side thrusters were used for the majority of maneuvers conducted in Lissajous orbit and were thus the primary focus of the calibration efforts.
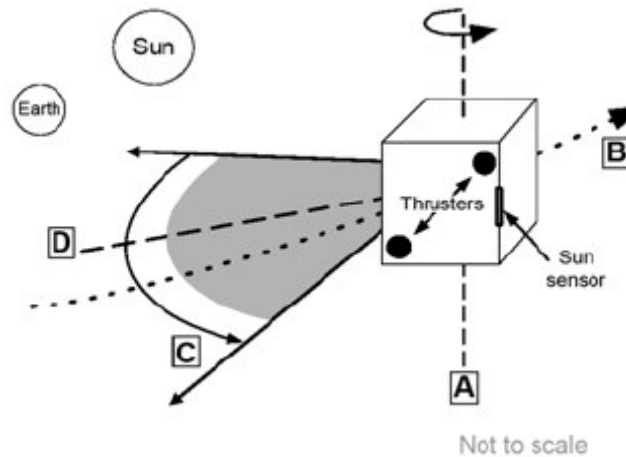
Figure 1. THEMIS/ARTEMIS spacecraft thrust pulse dynamics.[1] *This figure is a schematic of the spacecraft as it completes a thrust pulse. The spin axis is indicated by the dashed line labeled A; the path of travel is denoted by a dotted line marked B; the thrust arc is delineated with two solid arrows, a grey wedge, and an arrowed arc marked C; the centroid of thrust is the dashed line marked D.*

Because the spacecraft are always spinning, side-thrust maneuvers are performed in pulses as shown in Figure 1. These pulses have ranged from 32.5° to 60° in width.

The General Maneuver Program (GMAN) government-off-the-shelf software package is used to both plan and reconstruct THEMIS side-thrust maneuvers. GMAN takes multiple factors into account when predicting thruster performance (e.g., fuel tank pressure, thruster geometry, etc.), but ultimately a thruster scale factor is used to implicitly account for factors that are not explicitly considered (e.g., thruster catalyst bed efficiency, etc.).

The maneuver calibration process centers on determining the values for the thruster scale factors to use for planning and reconstructing each maneuver in order to reduce the discrepancy be-

tween actual and planned maneuver performance. Doing so ultimately conserves human effort and spacecraft propulsion resources by reducing the need for trajectory replanning and corrections due to such discrepancies. To conduct a side-thrust maneuver calibration, an analyst creates pre- and post-maneuver orbit solutions using tracking data and the Goddard Trajectory Determination System (GTDS). Then, the analyst feeds maneuver telemetry into two GMAN maneuver reconstruction iteration loops handled through an in-house software wrapper written in the Interactive Data Language (IDL). The first loop iterates on the difference between the thruster scale factors for both side thrusters in order to minimize the difference in the observed post-maneuver spacecraft spin rate and the reconstructed spin rate. The second iteration loop then varies the average thruster scale factor for both side-thrusters to minimize the difference between the observed change in an orbit metric (e.g., semi-major axis) over the course of the maneuver and the reconstructed change in that orbit metric.

As reported in (Reference 1), the initial phases of the calibration process uncovered a thruster scale factor dependence on the total amount of thruster on-time during a maneuver and differences in the thruster scale factors for the two side thrusters that ultimately lead to changes in the spacecraft spin rate over the course of a maneuver.

METHODS

The fundamentals of the thruster scale factor calibration process are described in detail in (Reference 1). However, as noted above, the unique demands of Lissajous orbit operations required several changes to this process. These updates are described in the remaining paragraphs of this section.

Functional Form Selection

The functional relationship of the thruster scale factor and total thruster on-time during a maneuver, x, as modeled in (Reference 1) is given as Eq. (1).[*] The derivative of this Eq. (1) is given as Eq. (2).

$$f(x) = B_0 \ln(x + B_1) + B_2 \tag{1}$$

$$f'(x) = \frac{B_0}{(x + B_1)} \tag{2}$$

This functional form produced adequate results for maneuvers conducted during the THEMIS primary mission and the orbit raising maneuver sequence of the low energy transfer to Lissajous orbit. However, as more data was collected during the initial Lissajous orbit stationkeeping maneuvers (SKMs), it became apparent that this functional form would produce unsatisfactory results for small maneuvers where the derivative of the function is at its largest values. Additionally, Eq. (1) produces undefined results whenever the sum of x and B_1 is less than or equal to zero. For example, a coefficient value of -1.49—which was the curve fit value determined by the lsqcurvefit Matlab function at the time that Eq. (1) was abandoned—would produce undefined results for maneuvers smaller than or equal to 1.49 seconds.

Thus, the functional form in Eq. (3) was ultimately implemented. When compared to Eq. (1), Eq. (3) produces better curve fits—as measured by the Mean Squared Error and Theil Inequality

---

[*] The notations used for equations in this paper are listed in the Notation section.

Statistics[1,4,5,6]—to the total maneuver dataset. Moreover, the coefficients of this form are outside of the logarithm terms and therefore the resulting thruster scale factor will be defined for all maneuver times greater than zero seconds.

$$f(x) = B_0 \log^2(x) + B_1 \log(x) + B_2 \tag{3}$$

ΔV Targeting

The calibration methods described in (Reference 1) relied on the comparison of the reconstructed and observed change to semi-major axis (SMA) magnitude caused by the maneuver. However, Keplerian elements such as the semi-major axis—which are useful for describing orbits that approximate those of a two-body system—are often rendered nonsensical by the multi-body dynamics that reign in the vicinity of the libration points. Thus, it was necessary to rely on the comparison of a non-Keplerian metric—the reconstructed and observed maneuver ΔV.

After applying ΔV as the comparison metric (i.e., ΔV Targeting) to the entire THEMIS/ARTEMIS side-thruster calibration data set, it was found that ΔV Targeting works best for maneuvers that occur in a regime in which the spacecraft does not travel through a significant arc of its orbit during the course of the maneuver. For example, when applied to medium-to-large maneuvers that occur near the periapses of highly elliptical orbits, ΔV Targeting produces inconsistent, nonsensical results for the thruster scale factor relative to SMA Targeting (e.g., 1.051 instead of 0.9364 for a 110 second long maneuver). However, for maneuvers occurring near apoapsis for highly elliptical orbits, in deep space, or in Lissajous orbit, ΔV Targeting produces more consistent and sensible results (e.g., 0.9337 instead of 0.9902 for a 73 second long maneuver).

The use of ΔV Targeting for some maneuvers and SMA Targeting for others presented a potential conundrum for maneuver planners as Lissajous orbit operations approached. At the time, it was recognized that ΔV would be the correct metric to use for Lissajous stationkeeping maneuver calibration, however, the data set of maneuvers for which ΔV Targeting was suitable was very small. Thus, it was not possible to use ΔV Targeting data alone to generate a decent curve fit to characterize the thruster scale factor's dependence on total thruster on-time during a maneuver. Fortunately the planners were able to include data points where SMA Targeting applied along with the ΔV Targeting data points in curve fits without any problems.

Figure 2. The combined ΔV and SMA Targeting calibration data for THEMIS B (ARTEMIS P1).
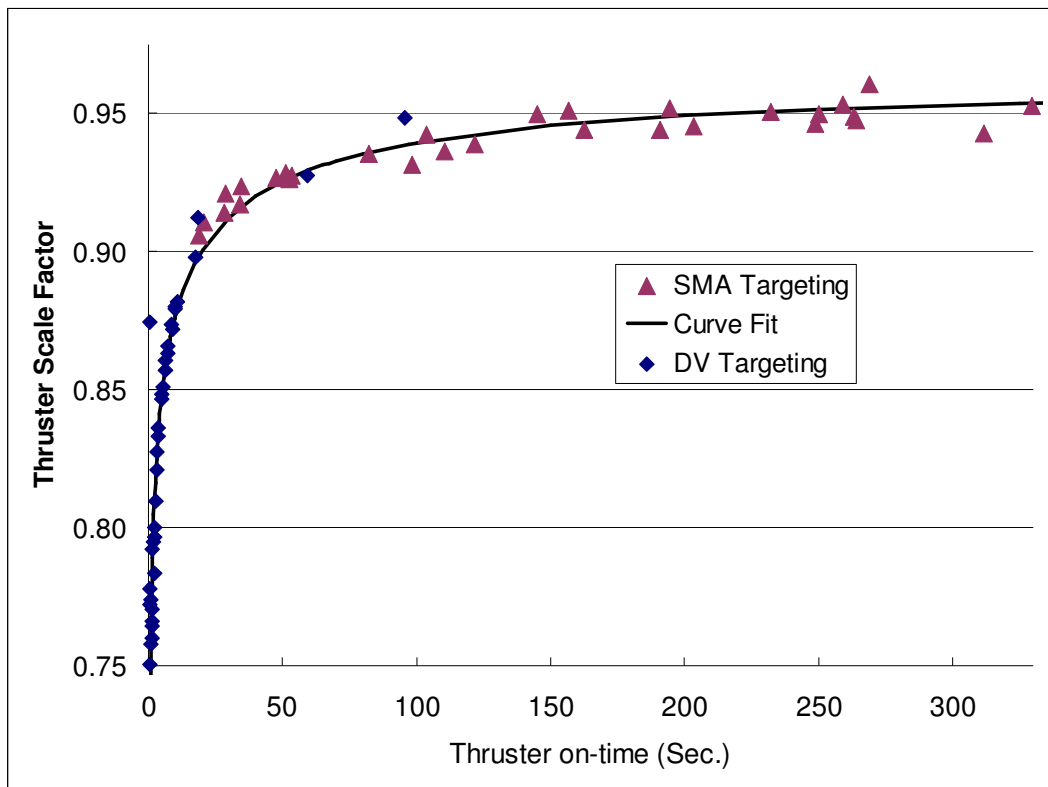
Figure 3. The combined Δ*V* and SMA Targeting data for THEMIS C (ARTEMIS P2).

As shown in Figure 2 and Figure 3 Δ*V* Targeting data can be used along with SMA Targeting data to produce an adequate curve fit.

CENDIS Targeting

Throughout the THEMIS primary mission and ARTEMIS low-energy transfer to Lissajous orbit, almost all of the calibrated side-thrust maneuvers were executed with a roughly 60° pulse width. However, as mentioned in (Reference 2), use of a pulse width of this size limited the minimum maneuver size to approximately 1.9 cm/s and introduced a significant maneuver execution error whenever the desired maneuver size was not a multiple of the minimum maneuver size. Thus, in order to perform the very small stationkeeping maneuvers that were required to minimize stationkeeping costs, the operations team began using different pulse widths—ranging from 32.5° to 60.04°—starting on SKM 10 for P1 and SKM 4 for P2. A total of 4 maneuvers were executed with a single pulse of the side-thrusters.

The implementation of the variable pulse width targeting introduced an error in the thrust direction equal to one-half the variation of the pulse from the previously nominal 60° pulse width. In other words, variation of the pulse width created a thrust centroid displacement (CENDIS) to be fed into GMAN that would create an error in the maneuver direction (i.e., phase) if not properly taken into account.

To characterize this CENDIS from flight data, it is necessary to compare the angle between the observed and targeted Δ*V* vectors projected into the spin plane (note that such comparisons are not very accurate when Δ*V* Targeting does not apply). First, the cross product of the spin axis

6

vector (i.e., the spacecraft attitude vector) and observed ΔV vectors is taken as shown in Eq. (4). Then the cross product of spin axis and targeted ΔV vector is taken as shown in Eq. (5).

$$\overline{A} \times \Delta \overline{V}_O = \overline{C}_O \tag{4}$$

$$\overline{A} \times \Delta \overline{V}_T = \overline{C}_T \tag{5}$$

These two cross products are in the spin plane, which is approximately parallel to the thrust vectors of the side-thrusters. Thus, the magnitude of the angle between these two cross products approximates the magnitude of the phase error. The direction of the phase error (i.e., whether the actual center of thrust of the pulse preceded or trailed the targeted center of thrust) is determined by taking the cross products of these cross products as shown in Eq. (6) and comparing its direction to that of the spin axis.

$$\overline{C}_T \times \overline{C}_O = \overline{C}_C \tag{6}$$

RESULTS

The calibration process (particularly with the aforementioned updates) was instrumental in the reduction of Lissajous orbit stationkeeping maneuver execution errors and detection of a mass ejection anomaly during Lissajous orbit operations. These results are described in the remainder of this section.

ΔV Magnitude Errors

The calibration process contributed to an overall decrease in ΔV magnitude errors and allowed the mission designers to decrease the targeted maneuver size throughout Lissajous orbit operations (refer to Tables 3 and 4 in the Appendix for the entire SKM data set). As shown in Table 1, the ΔV magnitude error decreased throughout Lissajous orbit operations, as the flight operation team gathered more calibration data and implemented techniques to reduce maneuver execution error. The average ΔV magnitude error prior to the implementation of Variable Pulse Width (VPW) maneuver planning and execution was 6.724 mm/s; after the implementation of VPW, the average ΔV magnitude error fell to 1.146 mm/s. Over the final 10 Lissajous stationkeeping maneuvers, the average and median ΔV magnitude errors were 0.9042 mm/s and 0.6642 mm/s, respectively. The minimum maneuver magnitude error was 46.3 µm/s.

Table 1. ΔV Magnitude Error Statistics for Several Subsets of ARTEMIS Lissajous Stationkeeping Maneuvers.

Maneuver Set (Year/DOY)	Number of Lissajous Orbit Stationkeeping Maneuvers	Minimum Targeted ΔV Magnitude (m/s)	Maximum Targeted ΔV Magnitude (m/s)	Average ΔV Magnitude Error (m/s)	Median ΔV Magnitude Error (m/s)
2011/124 – 2011/169	10	0.011696	0.130	9.042×10^{-4}	6.642×10^{-4}
2011/075 – 2011/169	23	"	0.279	9.916×10^{-4}	7.252×10^{-4}
2011/006 – 2011/169	39	"	0.296	1.079×10^{-3}	7.252×10^{-4}
2010/315 – 2011/169	51	"	0.349	1.146×10^{-3}	8.169×10^{-4}
2010/237 – 2011/169	63	"	2.562	2.166×10^{-3}	1.162×10^{-3}
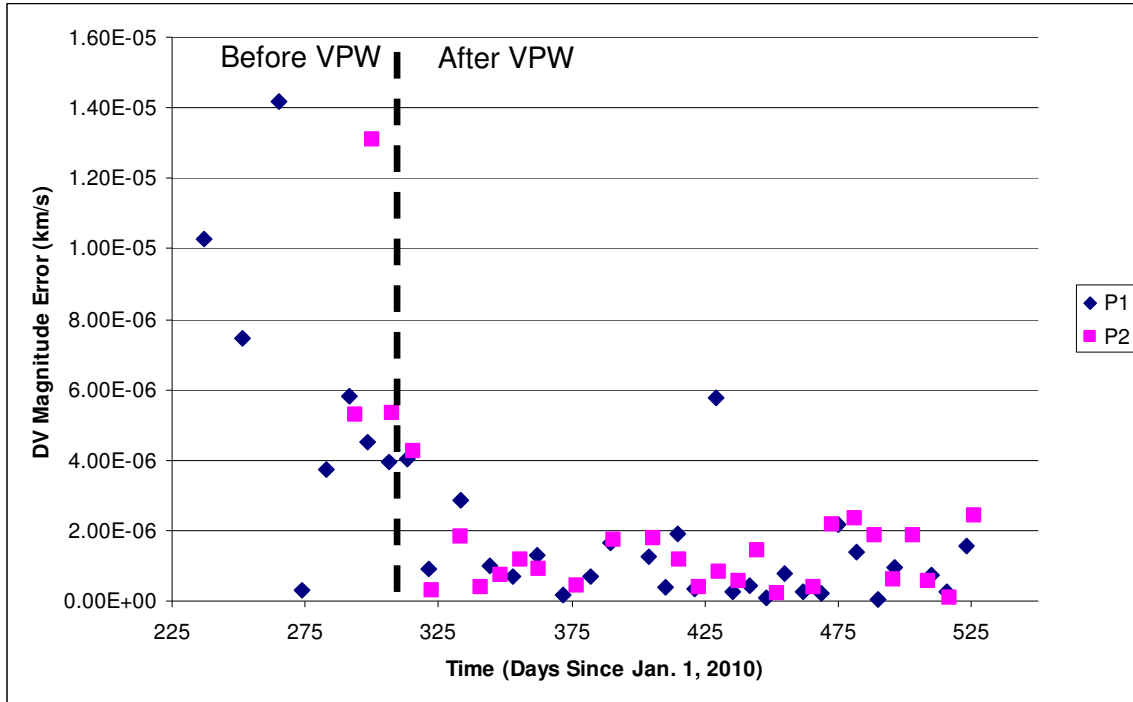
Figure 4. The time history of the ΔV magnitude error during ARTEMIS Lissajous orbit operations with a line denoting when Variable Pulse Width (VPW) targeting and execution was implemented.

Figure 4 contains the time history of the ΔV magnitude error for the Lissajous orbit station-keeping maneuvers. This figure further demonstrates the drop in magnitude errors associated with the improvements to the calibration process and the implementation of VPW maneuver planning and execution.

Time between Stationkeeping Maneuvers

Due to the unstable dynamics of Lissajous orbits, maneuver navigation and execution errors can cause the actual trajectory of the spacecraft to diverge significantly from its desired trajectory over time. Thus, these errors effectively dictate the allowable time between stationkeeping maneuvers. Throughout ARTEMIS Lissajous orbit operations, the calibration process helped to keep maneuver execution errors low enough to give mission designers the option of experimenting with the time between stationkeeping maneuvers. The minimum time between maneuvers was 4.6 days and the maximum time between maneuvers was 14.273 days. Ultimately, the mission designers concluded that ΔV costs can be optimized by reducing the time between maneuvers and keeping them close to the Earth-Moon line crossing[3]—which occurred roughly every seven days—and thus the average time between stationkeeping maneuvers was 8.07 days.

Pulse Phasing Errors

The pulse phasing error (i.e., the thrust centroid displacement or CENDIS) due to GMAN's modeling of the thrust centroid and variation of the pulse width is more observable on maneuvers where ΔV Targeting applies than it is on maneuvers where SMA Targeting applies. Unfortunately, only a few of these maneuvers were conducted before the Lissajous orbit insertions for P1

8

and P2. Moreover, almost all maneuvers prior to the Lissajous orbit insertions were conducted at a pulse width of 60°. Thus, the errors were not anticipated by the operations team and were fairly large for the first few stationkeeping maneuvers. Workable calibration curves (i.e., linear functions of pulse width) for the CENDIS were derived and implemented in time for SKM 16 for P1 and SKM 12 for P2.
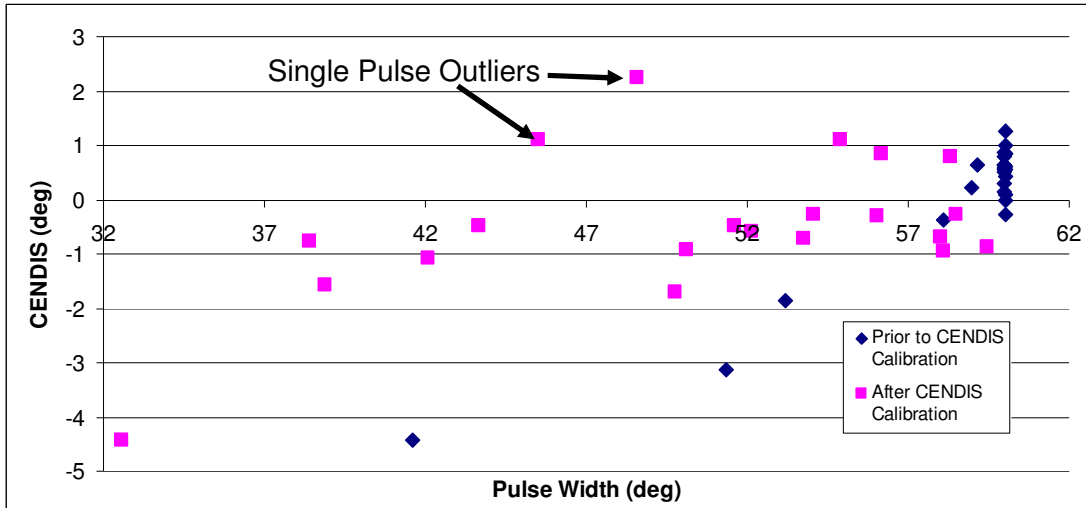
Figure 5. ARTEMIS P1 CENDIS for maneuvers between initial lunar flyby targeting and lunar orbit insertion.
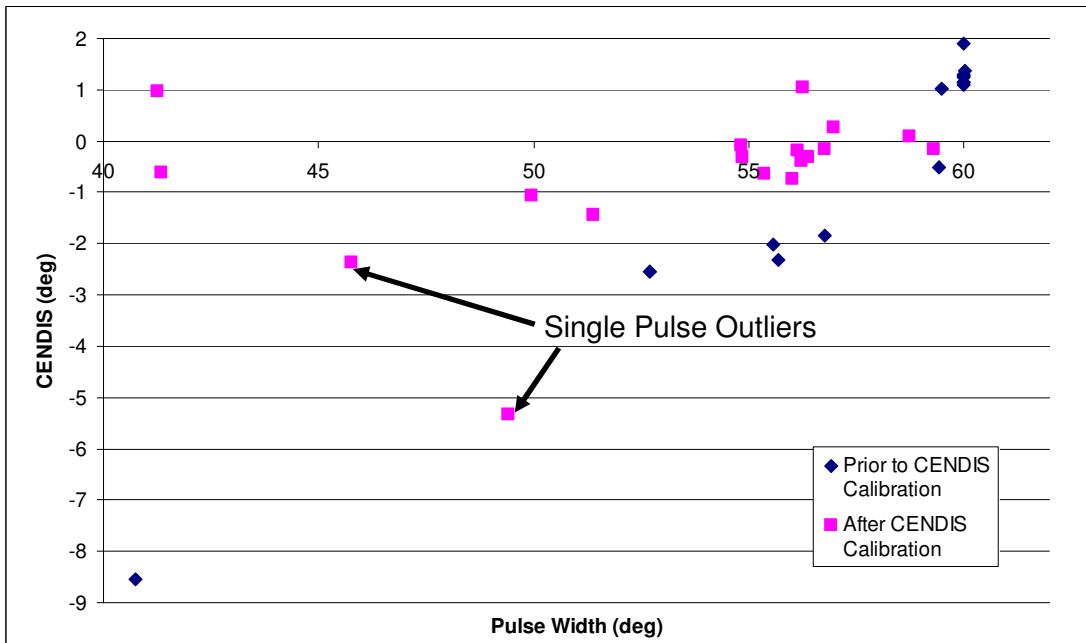
Figure 6. ARTEMIS P2 CENDIS for maneuvers between initial lunar flyby targeting and lunar orbit insertion

As shown in Figure 5 and Figure 6, the CENDIS calibration effort reduced pulse phasing errors to average magnitudes of 0.99° and 0.78° for P1 and P2, respectively, for multi-pulse maneuvers. For single pulse maneuvers, the pulse phasing errors remained relatively high, perhaps due to limitations in generating or measuring the thrust vector for maneuvers that small in magnitude.

ARTEMIS P1 instrument sphere loss anomaly

On October 14, 2010, a 0.092 kg instrument sphere unexpectedly detached from ARTEMIS P1 and imparted a 5.67 cm/s ΔV on the spacecraft.[7,8] As mentioned in (Reference 7), the operations team was first alerted to this anomaly when a calibration run failed to converge on a value for the thruster scale factor after having converged on a reasonable value the previous two days. Had this particular anomaly occurred at a time when calibration runs were not being conducted, the anomaly probably would have gone unnoticed until the automated orbit determination run on the following day.

After the anomaly, the spacecraft's spin down rate increased dramatically. The calibrated thrust offset went from -0.000838 on P1 SKM 5 to -0.04022 on P1 SKM 6. Moreover, the relationship between the thruster scale factor and thruster on-time curve changed due to a peculiarity in GMAN. In GMAN the thruster I_{SP} for each pulse drops as the spin rate drops over a maneuver segment. Because the spacecraft now spins down faster over a given maneuver segment, GMAN will lower its performance estimates for that segment and one would have to use a higher thruster scale factor for the maneuver to compensate. While this effect was negligible (and unnoticed) during the remaining stationkeeping maneuvers due to their small size, it ultimately led to roughly 6% overburn on the lunar orbit insertion.

FUTURE WORK

Now that ARTEMIS Lissajous orbit operations have ceased and both spacecraft are in stable lunar orbits, all foreseeable maneuvers in the future will be calibrated through SMA Targeting. Additionally, the operations team will continue updating the calibration process in response to anomalies encountered by the ARTEMIS and THEMIS-Low spacecraft. For example, the new spin-down characteristics for P1 will require a significant update to the calibration curve particularly in the large maneuver regime.

CONCLUSION

The updates to the calibration process prior to and during Lissajous orbit operations helped to keep stationkeeping costs low by reducing the magnitude of ΔV and pulse phasing errors during maneuver execution. Additionally, the process allowed mission designers to experiment with the timing of stationkeeping maneuvers and alerted the mission operations team to a significant anomaly on P1. These results underscore the importance of establishing and continually updating maneuver performance calibration processes during operations, particularly when government-off-the-shelf and commercial-off-the-shelf software packages are used for maneuver planning. The use of such packages provides maneuver planners with little insight into the inner workings of the software and how it will work in novel situations, such as Lissajous orbit stationkeeping. Accordingly, maneuver planners will sometimes be caught by surprise in such situations—as exemplified by the large CENDIS for the early stationkeeping maneuvers and the overburn on the P1 lunar orbit insertion. However, as demonstrated during the THEMIS and ARTEMIS missions, careful attention to maneuver performance calibration can help to minimize both the short-term and long-term effects of these types of surprises so that maneuver planners will be free to continue pushing the envelope of spacecraft trajectory design.

ACKNOWLEDGMENTS

NOTATION

$\overline{A}$ Spacecraft attitude vector (spin axis vector)

B_0 First curve fit coefficient

B_1 Second curve fit coefficient

B_2 Third curve fit coefficient

$\overline{C}_C$ Cross product of the attitude and spacecraft velocity change vectors cross products

$\overline{C}_O$ Cross product of attitude and observed spacecraft velocity change vectors

$\overline{C}_T$ Cross product of attitude and observed spacecraft velocity change vectors

I_{SP} Specific impulse

x Total thruster on-time for a maneuver (in seconds)

ΔV Change in spacecraft velocity

$\Delta \overline{V}_O$ Vector for observed change in spacecraft velocity

$\Delta \overline{V}_T$ Vector for targeted change in spacecraft velocity

APPENDIX

The table in this appendix contains maneuver size and error statistics for all of the ARTEMIS stationkeeping maneuvers.

Table 2. Maneuver size and error statistics for ARTEMIS P1's Lissajous stationkeeping maneuvers.

Maneuver ID	Time of First Thruster Pulse	Number of Pulses/ Pulse Width (deg)	Targeted ΔV Magnitude (km/s)	ΔV Magnitude Error (km/s)	ΔV Magnitude Error (%)
SKM 36	11/157 19:40:03	3/49.78	4.03E-05	1.56E-06	3.88%
SKM 35	11/150 20:40:01	1/45.49	1.17E-05	2.67E-07	2.29%
SKM 34	11/144 15:54:56	4/50.11	5.53E-05	7.25E-07	1.31%
SKM 33	11/131 07:19:56	4/54.91	6.04E-05	9.48E-07	1.57%
SKM 32	11/124 14:14:49	8/56.04	1.30E-04	4.63E-08	-0.04%
SKM 31	11/116 16:45:03	2/53.76	2.78E-05	1.39E-06	5.00%
SKM 30	11/110 01:59:40	16/58.49	2.79E-04	2.16E-06	0.77%
SKM 29	11/103 10:30:01	2/42.11	2.17E-05	2.19E-07	1.01%
SKM 28	11/096 18:54:59	2/38.88	1.97E-05	2.59E-07	-1.31%
SKM 27	11/089 19:09:59	2/38.40	2.04E-05	7.70E-07	-3.77%
SKM 26	11/083 02:35:02	2/43.66	2.32E-05	1.07E-07	-0.46%
SKM 25	11/076 10:25:01	2/32.58	1.74E-05	4.35E-07	-2.50%
SKM 24	11/070 03:44:58	2/56.18	2.93E-05	2.60E-07	-0.89%
SKM 23	11/063 23:59:59	2/32.87	1.76E-05	5.77E-06	32.85%
SKM 22	11/056 04:19:59	4/54.05	5.93E-05	3.33E-07	0.56%
SKM 21	11/049 20:45:02	1/48.57	1.17E-05	1.93E-06	16.45%
SKM 20	11/045 06:09:52	7/51.59	1.03E-04	3.78E-07	0.37%
SKM 19	11/038 19:04:45	13/58.08	2.23E-04	1.24E-06	0.56%
SKM 18	11/032 18:34:31	N/A (Axial Thrusters)	N/A	N/A	N/A
SKM 17	11/024 07:59:56	4/58.32	6.38E-05	1.66E-06	-2.60%
SKM 16	11/017 06:55:00	8/52.12	1.19E-04	6.75E-07	0.57%
SKM 15	11/006 18:40:03	3/41.62	3.35E-05	1.60E-07	-0.48%
SKM 14	10/361 17:15:03	7/58.08	1.16E-04	1.30E-06	1.13%
SKM 13	10/352 14:30:04	9/53.19	1.38E-04	6.99E-07	0.51%
SKM 12	10/344 06:30:05	13/58.97	2.26E-04	9.84E-07	0.43%
SKM 11	10/334 05:55:03	12/59.17	2.07E-04	2.86E-06	1.38%
SKM 10	10/321 08:45:03	5/51.36	7.13E-05	9.03E-07	1.27%
SKM 9	10/313 01:45:03	4/60.01	6.96E-05	4.04E-06	-5.81%
SKM 8	10/306 04:59:53	7/60.00	1.16E-04	3.95E-06	3.39%
SKM 7	10/298 06:59:51	7/60.01	1.13E-04	4.52E-06	4.00%
SKM 6	11/157 19:40:03	9/49.78	1.58E-04	5.79E-06	-3.67%
SKM 5	10/282 16:30:05	5/60.01	7.81E-05	3.72E-06	4.77%
SKM 4	10/273 16:24:33	19/59.99	3.41E-04	2.92E-07	-0.09%
SKM 3	10/265 08:59:44	12/60.04	2.23E-04	1.42E-05	-6.37%
SKM 2	10/251 10:59:15	32/59.99	5.84E-04	7.47E-06	1.28%
SKM 1	10/237 04:26:41	135/59.98	2.56E-03	1.03E-05	0.40%

Table 3. Maneuver size and error statistics for ARTEMIS P2's Lissajous stationkeeping maneuvers.

Maneuver ID	Time of First Thruster Pulse	Number of Pulses/ Pulse Width (deg)	Targeted ΔV Magnitude (km/s)	ΔV Magnitude Error (km/s)	ΔV Magnitude Error (%)
SKM 31	11/161 04:00:01	4/56.27	6.78E-05	2.41E-06	-3.55%
SKM 30	11/152 00:05:00	2/41.25	2.43E-05	7.46E-08	0.31%
SKM 29	11/143 17:05:00	1/49.42	1.45E-05	5.65E-07	3.91%
SKM 28	11/138 02:05:00	2/32.55	1.91E-05	1.84E-06	-9.63%
SKM 27	11/130 18:35:00	2/39.96	2.35E-05	6.03E-07	2.57%
SKM 26	11/123 17:29:57	4/56.97	6.85E-05	1.88E-06	-2.75%
SKM 25	11/116 04:15:01	1/45.77	1.33E-05	2.33E-06	17.55%
SKM 24	11/107 10:54:57	3/51.40	4.53E-05	2.18E-06	-4.82%
SKM 23	11/100 20:09:57	3/56.02	4.96E-05	3.93E-07	0.79%
SKM 22	11/086 20:29:58	2/34.00	1.99E-05	2.24E-07	1.13%
SKM 21	11/079 10:45:01	3/49.96	4.38E-05	1.41E-06	-3.23%
SKM 20	11/072 22:29:43	12/54.84	2.11E-04	5.60E-07	-0.27%
SKM 19	11/065 06:49:43	12/56.22	2.16E-04	8.17E-07	-0.38%
SKM 18	11/057 17:00:03	3/41.34	3.63E-05	4.01E-07	-1.10%
SKM 17	11/050 02:19:45	10/55.35	1.74E-04	1.16E-06	-0.67%
SKM 16	11/040 08:34:38	16/56.78	2.96E-04	1.78E-06	-0.60%
SKM 15	11/032 02:09:59	N/A (Axial Thrusters)	N/A	N/A	N/A
SKM 14	11/025 10:04:44	10/56.39	1.78E-04	1.73E-06	-0.97%
SKM 13	11/018 13:48:46	N/A (Axial Thrusters)	N/A	N/A	N/A
SKM 12	11/011 20:40:01	7/54.86	1.19E-04	4.17E-07	0.35%
SKM 11	11/004 16:43:35	N/A (Axial Thrusters)	N/A	N/A	N/A
SKM 10	10/362 16:25:03	7/55.57	1.21E-04	9.15E-07	0.75%
SKM 9	10/355 12:40:03	3/40.74	3.69E-05	1.19E-06	-3.23%
SKM 8	10/348 03:40:00	4/55.69	6.64E-05	7.16E-07	-1.08%
SKM 7	10/340 22:55:03	6/56.78	1.04E-04	3.80E-07	-0.37%
SKM 6	10/333 04:45:04	18/59.44	3.48E-04	1.84E-06	0.53%
SKM 5	10/322 05:25:04	4/52.72	6.29E-05	3.25E-07	-0.52%
SKM 4	10/315 10:50:05	13/59.48	2.52E-04	4.23E-06	-1.68%
SKM 3	10/307 14:04:31	19/60.01	3.79E-04	5.34E-06	-1.41%
SKM 2	10/300 06:14:46	9/60.01	1.84E-04	1.31E-05	-7.13%
SKM 1	10/293 12:50:04	6/59.99	1.17E-04	5.31E-06	-4.54%

REFERENCES

[1] Marchese, J. E., Owens, B. D., Cosgrove, D., Frey, S., and Bester, M., "Calibration of In-flight Maneuver Performance for the THEMIS and ARTEMIS Mission Spacecraft," *Proceedings of the AIAA 2010 SpaceOps Conference*, Huntsville, AL, April 25-30, 2010.

[2] Cosgrove, D., Frey, S., Folta, D., Woodard, M., Woodfork, D., Marchese, J. E., Owens, B. D., Gandhi, S., and Bester, M., "Navigating THEMIS to the ARTEMIS Low-Energy Lunar Transfer Trajectory," *Proceedings of the AIAA 2010 SpaceOps Conference*, Huntsville, AL, April 25-30, 2010.

[3] Folta, D. C., Woodard, M. A., Cosgrove, D., "Stationkeeping of the First Earth-Moon Libration Orbiters: The ARTEMIS Mission," *Proceedings of the 2011 AAS/AIAA Astrodynamics Specialists Conference*, Jul. 31-Aug. 4, Girdwood, AK.

[4] Sterman, J. D., "Appropriate Summary Statistics for Evaluating the Historical Fit of System Dynamics Models," *Dynamica*, Vol. 10, No. 2, 1984, pp. 51-66.

[5] Sterman, J. D., *Business Dynamics: Systems Thinking and Modeling for a Complex World*, Irwin/McGraw-Hill, New York, 2000, pp. 874-880.

[6] Theil, H., *Applied Economic Forecasting*, North Holland Publishing Company, Amsterdam, 1966.

[7] Owens, B. D., Cosgrove, D. P., Marchese, J. E., Bonnell, J. W., Pankow, D. H., Frey, S., Bester, M.G., "Mass Ejection Anomaly in Lissajous Orbit: Response and Impliciations for the ARTEMIS Mission," *Proceedings of the 22nd AAS/AIAA Space Flight Mechanics Meeting,* Charleston, SC, Jan. 29 – Feb. 2, 2012.

[8] Woodard, M.; D. Folta; D. Cosgrove; J. Marchese; B. Owens; and P. Morinelli (2011), "Orbit Determination ofSpacecraft in Earth-Moon L1 and L2 Libration Point Orbits," *Proceedings of the 2011 AAS/AIAA Astrodynamics Specialists Conference*, Jul. 31-Aug. 4, Girdwood, AK.